Arab J Sci Eng (2016) 41:4359–4369
DOI 10.1007/s13369-016-2132-4

RESEARCH ARTICLE - MECHANICAL ENGINEERING

Wave Characteristics of Nanotubes Conveying Fluid Based on the Non-classical Timoshenko Beam Model Incorporating Surface Energies

R. Ansari[1] · R. Gholami[2] · A. Norouzzadeh[1] · M. A. Darabi[1]

Received: 8 July 2015 / Accepted: 21 March 2016 / Published online: 1 April 2016
© King Fahd University of Petroleum & Minerals 2016

Abstract The aim of this paper was to investigate the wave propagation of nanotubes conveying fluid by considering the surface stress effect. To this end, the nanotube is modeled as a Timoshenko nanobeam. According to the Gurtin–Murdoch continuum elasticity, the surface stress effect is incorporated into the governing equations of motion obtained from the Hamilton principle. The governing differential equations are solved by generalized differential quadrature method. Then, the effects of the thickness, material and surface stress modulus, residual surface stress, surface density and flow velocity on spectrum curves of nanotubes predicted by both classical and non-classical theories are studied. The first three fundamental modes including flexural, axial, and shear waves of nanotubes are considered.

Keywords Fluid-conveying nanotubes · Timoshenko beam theory · Wave propagation · Surface stress · Gurtin–Murdoch elasticity continuum · Generalized differential quadrature method

List of symbols

Nanotube

L	Length (m)
h	Thickness (m)
d_i	Inner diameter (m)
d_o	Outer diameter (m)
E	Young's modulus (Pa)
ν	Poisson's ratio
λ, μ	Lame's constants (Pa)
ρ	Mass density (kg/m^3)
A	Cross-sectional area (m^2)
I	Second moment of inertia (m^4)

Fluid flow

ρ_f	Mass density (kg/m^3)
V	Velocity (m/s)
A_f	Cross-sectional area (m^2)
I_f	Second moment of inertia (m^4)

Solution

(U, W, Ψ)	Amplitude of displacement field
k	Wave number
ω	Frequency
$\mathbf{M}$	Inertia matrix
$\mathbf{C}$	Damping matrix
$\mathbf{K}$	Stiffness matrix
$\mathbf{I}$	Identity matrix
$\mathbf{S}$	State-space matrix

✉ R. Gholami
gholami_r@liau.ac.ir

R. Ansari
r_ansari@guilan.ac.ir

[1] Department of Mechanical Engineering, University of Guilan, P.O. Box 3756, Rasht, Iran

[2] Department of Mechanical Engineering, Lahijan Branch, Islamic Azad University, P.O. Box 1616, Lahijan, Iran

Surface layers

E_s	Elasticity modulus (Pa)
ν_s	Poisson's ratio
ρ_s	Mass density (kg/m^2)
τ_s	Residual tension (N/m)
λ_s, μ_s	Lame's constants (N/m)

Formulation

(x, y, z)	Cartesian coordinate system
(u, w, ψ)	Displacement field $(m, m, -)$
ε_{xx}	Strain
$\sigma_{ij}, \sigma^s_{ij}$	Stresses (Pa, N/m)
$N_{xx}, \bar{N}_{xx}$	Resultant normal forces (N)
$M_{xx}, \bar{M}_{xx}$	Resultant bending moments (Nm)
$Q_x, \bar{Q}_x$	Resultant shear forces (N)
Π_s	Strain energy (J)
Π_T	Kinetic energy (J)
Π_{T_f}	Fluid kinetic energy (J)
$A_{11}, A_{33}, A_{55}; D_{11}, E_{11}$	Stiffness components (in Eq. 15) (N; Nm^2)
$I_0; I_2, G$	Inertia components (in Eq. 15) (kg/m; kg m)
$u, w, x, \eta, \tau, I_0^*, I_2^*, g, a_{11}$	Non-dimensional parameters
$a_{13}, a_{33}, d_{11}, e_{11}, K_b, v$	(in Eq. 17)

1 Introduction

Tubular nanomaterials have aroused intense attention since carbon nanotubes were discovered by Iijima in 1991 [1]. The stupendous and elevated mechanical, electronic and optical properties of these structures provide a wide spectrum of prospective applications in nanomechanics, catalysts, pharmaceuticals, and nanoelectronics [2–6].

Applications of tubular nanomaterials in nanofluidic systems like the fluid storage, fluid transport, and drug delivery are other fulfilling features of these nanostructures [7–11]. In order to use all potential applications of fluid-conveying hollow cylinders and achieve maximum efficiency, it is of high importance to investigate concerning mechanical phenomena in terms of static and dynamic behavior. From theoretical point of view, generally studies can be performed in two categories, namely classical and non-classical continuum theories. Small-scale effect, an inherent nature of nano- and microstructures, has been demonstrably approved to have significant effect on the mechanical response [12–18]. Several non-classical continuum-based theories capable of capturing scale dependency have been represented such as the strain gradient elasticity, couple stress elasticity, nonlocal elasticity and the surface elasticity theories [19–22,25]. In this regard, it can be pointed to the work of Ghayesh [26] who studied the nonlinear forced oscillations of single-walled carbon nanotubes with the help of nonlocal elasticity theory for the primary and superharmonic excitations.

One of the most successful models to consider the surface stress effect was the one proposed by the Gurtin and Murdoch [27,28] which the accuracy of their results are comparable to those of atomistic models. According to their proposition, the surface layer of a solid can be treated as a mathematical layer with zero thickness and different material characteristics from the underlying bulk which is completely surrounded by the membrane. The surface properties of a solid are anisotropic and reliant on crystallographic direction of the surface, so surfaces are due to anisotropic stresses [29,30]. However, suitable averages of surface stress can be used to estimate isotropic stresses for the surface [31,32]. Only a few studies have been accomplished to consider surface stress effect on the vibration and wave characteristics of fluid-conveying nanotubes. In this respect, Wang [33] studied the vibration behavior of nanotubes conveying fluids with consideration of the surface effect. He reported that small tubes with large aspect ratios have significant effect on the stability of the nanotubes.

In current paper, the effect of the surface stress on the wave characteristics of fluid-conveying nanotubes is investigated. The nanotube is considered to be modeled based on the Timoshenko beam theory. The governing equations of motion incorporating the surface stress effect are achieved based on the Hamilton principle and Gurtin–Murdoch continuum elasticity. Effects of the thickness, material, and surface stress modulus, residual surface stress, surface density and flow velocity on the first three fundamental modes including flexural, axial and shear waves of nanotubes predicted by both classical and non-classical theories are investigated.

2 Formulation of Motion

Shown in Fig. 1 is a schematic of a nanotube with length L and thickness h, conveying incompressible fluid of the mass density ρ_f, flowing with constant velocity V. So as to simulate the internal flow a continuum-based plug-like flow is used. It is considered that the outside of the nanotube contains a bulk part and two additional thin surface layers (inner and outer layers). The properties of the bulk part are Young's modulus E, Poisson's ratio ν, and mass density ρ. d_i and d_o are the symbols to denote the inner and outer diameters, respectively. The two surface layers have following properties: surface elasticity modulus of E_s, Poisson's ratio ν_s, mass density ρ_s, and the surface residual tension τ_s.

The Cartesian coordinate system (x, y, z) with the x-axis along the length of the deflected nanotube, the y-axis along the neutral axis and the z-axis along the transverse direc-

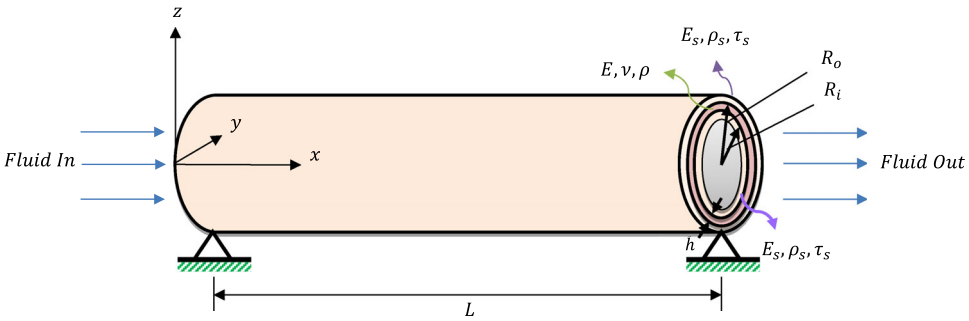

Fig. 1 Geometry of fluid-conveying nanotube with two surface layers

tion is considered in one end of the nanotube. Based on the first-order shear deformation Timoshenko beam theory, the displacements of an arbitrary point in the nanobeam along the x-, y-, and z-axes can be written in a general form as

$$u_x = u(x,t) + z\psi(x,t), \qquad u_y = 0, \qquad u_z = w(x,t) \tag{1}$$

where $u(x,t)$, $w(x,t)$ and $\psi(x,t)$ denote the axial displacement of the center of sections, the lateral deflection of the nanotube, and the rotation angle of the cross section with respect to the vertical direction, respectively.

The strain–displacement relations can be written as

$$\varepsilon_{xx} = \frac{\partial u}{\partial x} + z\frac{\partial \psi}{\partial x}, \varepsilon_{xz} = \frac{1}{2}\left(\frac{\partial w}{\partial x} + \psi\right) \tag{2}$$

Also, the stress components can be expressed according to the linear elasticity as follows

$$\sigma_{xx} = (\lambda + 2\mu)\left(\frac{\partial u}{\partial x} + z\frac{\partial \psi}{\partial x}\right), \quad \sigma_{xz} = \mu\left(\frac{\partial w}{\partial x} + \psi\right) \tag{3}$$

in which $\lambda = E\nu/\left(1-\nu^2\right)$ and $\mu = E/(2(1+\nu))$ are Lame's constants. The classical continuum mechanics is incapable of capturing the atomic features of the nanostructures. The Gurtin–Murdoch theory is a modified continuum elasticity to consider the scale dependency. On account of the interaction between the elastic surface and the bulk material, nanostructures is undergoing in-plane loads in different directions, causing surface stresses. According to the Gurtin–Murdoch theory, these surface stresses can be computed by employing following surface constitutive equations

$$\begin{aligned} &\sigma^s_{\alpha\beta} = \tau_s\delta_{\alpha\beta} + (\tau_s + \lambda_s)\varepsilon_{\gamma\gamma}\delta_{\alpha\beta} + 2(\mu_s - \tau_s)\varepsilon_{\alpha\beta} + \tau_s u^s_{\alpha,\beta}; \\ &\sigma^s_{\alpha z} = \tau_s u^s_{z,\alpha} \\ &(\alpha, \beta = x, y) \end{aligned} \tag{4}$$

here λ_s and μ_s are Lame's surface constants. The surface stress components can be written with respect to the displacement components as

$$\sigma^s_{xx} = (\lambda_s + 2\mu_s)\left(\frac{\partial u}{\partial x} + z\frac{\partial \psi}{\partial x}\right) + \tau_s, \quad \sigma^s_{xz} = \tau_s\frac{\partial w}{\partial x} \tag{5}$$

In the classical theory, the stress component σ_{zz} is considered to be zero, since it is negligible compared to the σ_{xx} and σ_{xz}. This assumption does not fulfill surface conditions of the Gurtin–Murdoch model. To satisfy the balance conditions on the surfaces, the stress component σ_{zz} is assumed to be linearly variable through the beam thickness, i.e., [34]

$$\begin{aligned} \sigma_{zz} = &\frac{\left(\frac{\partial \sigma^{s+}_{xz}}{\partial x} - \rho^{s+}\frac{\partial^2 w}{\partial t^2}\right) - \left(\frac{\partial \sigma^{s-}_{xz}}{\partial x} - \rho^{s-}\frac{\partial^2 w}{\partial t^2}\right)}{2} \\ &+ \frac{\left(\frac{\partial \sigma^{s+}_{xz}}{\partial x} - \rho^{s+}\frac{\partial^2 w}{\partial t^2}\right) + \left(\frac{\partial \sigma^{s-}_{xz}}{\partial x} - \rho^{s-}\frac{\partial^2 w}{\partial t^2}\right)}{h} z \end{aligned} \tag{6}$$

Referring to Eq. (5), σ_{zz} can be obtained as

$$\sigma_{zz} = \frac{2z}{h}\left(\tau_s\frac{\partial^2 w}{\partial x^2} - \rho_s\frac{\partial^2 w}{\partial t^2}\right) \tag{7}$$

Inserting σ_{zz} achieved from Eq. (7) in the components of stress for the bulk of the nanotube leads to following relations

$$\begin{aligned} \sigma_{xx} = &(\lambda + 2\mu)\left(\frac{\partial u}{\partial x} + z\frac{\partial \psi}{\partial x}\right) \\ &+ \frac{2\nu z}{(1-\nu)h}\left(\tau_s\frac{\partial^2 w}{\partial x^2} - \rho_s\frac{\partial^2 w}{\partial t^2}\right), \\ \sigma_{xz} = &\mu\left(\frac{\partial w}{\partial x} + \psi\right). \end{aligned} \tag{8}$$

According to the continuum surface elasticity theory, the strain energy of the nanotube incorporating the surface stress effect can be written as

$$\begin{aligned} \Pi_s = &\frac{1}{2}\int_x\int_A \sigma_{ij}\varepsilon_{ij}\mathrm{d}A\mathrm{d}x \\ &+ \frac{1}{2}\left(\int_{S^+}\sigma^s_{ij}\varepsilon_{ij}\mathrm{d}S^+ + \int_{S^-}\sigma^s_{ij}\varepsilon_{ij}\mathrm{d}S^-\right) \end{aligned}$$

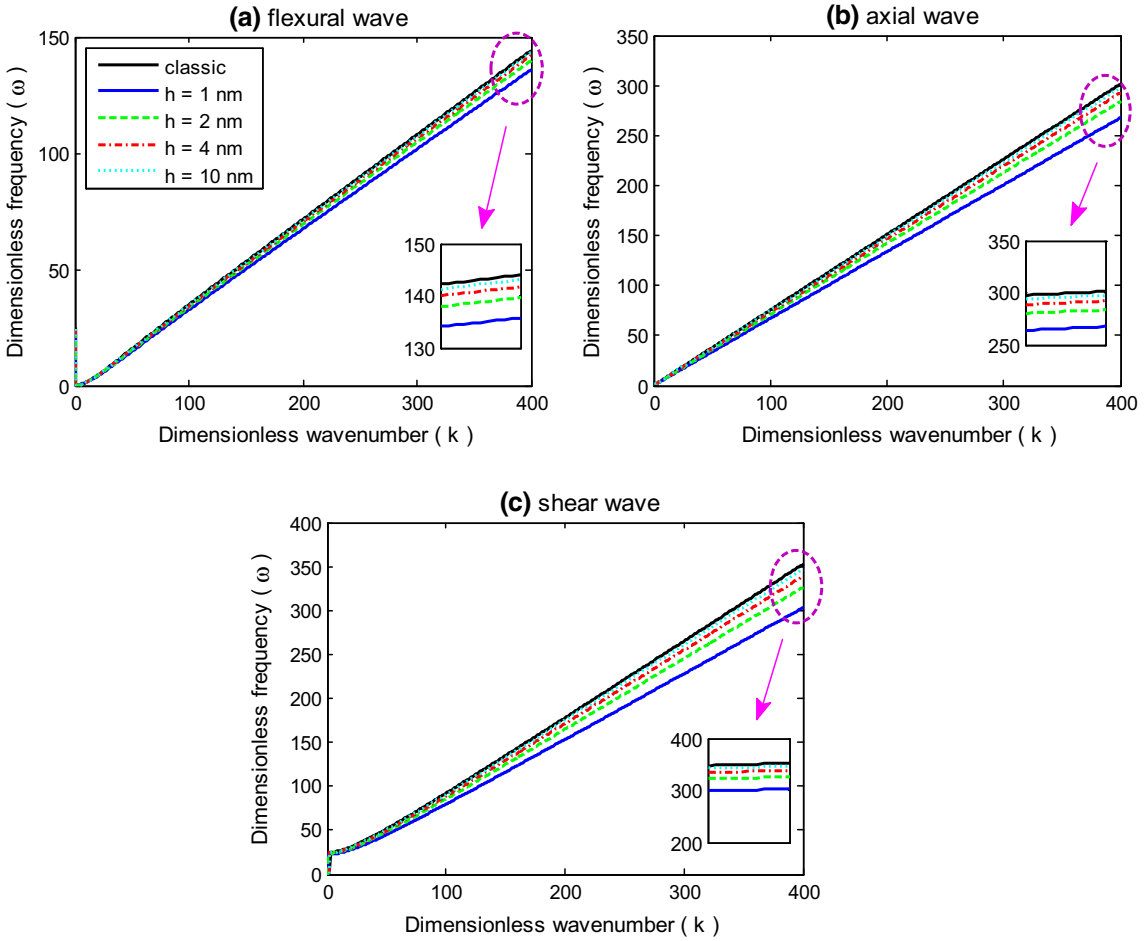

Fig. 2 Dispersion curves for different values of thicknesses corresponding to flexural, axial, and shear waves

$$= \frac{1}{2}\int_x \left\{ \left(N_{xx} + \bar{N}_{xx}\right)\frac{\partial u}{\partial x} + \left(M_{xx} + \bar{M}_{xx}\right)\frac{\partial \psi}{\partial x} + Q_x\left(\frac{\partial w}{\partial x} + \psi\right) + \bar{Q}_x\frac{\partial w}{\partial x}\right\} \mathrm{d}x \tag{9}$$

in which

$$N_{xx} = (\lambda + 2\mu)\, A\frac{\partial u}{\partial x},\ Q_x = \mu k_\mathrm{s} A\left(\frac{\partial w}{\partial x} + \psi\right),$$
$$M_{xx} = (\lambda + 2\mu)\, I\frac{\partial \psi}{\partial x} + \frac{2\nu I}{(1-\nu)\, h}\left(\tau_\mathrm{s}\frac{\partial^2 w}{\partial x^2} - \rho_\mathrm{s}\frac{\partial^2 w}{\partial t^2}\right). \tag{10a}$$

$$\bar{N}_{xx} = \int_S \sigma^s_{xx}\mathrm{d}s = \pi\left(d_\mathrm{i} + d_\mathrm{o}\right)\left(\lambda_\mathrm{s} + 2\mu_\mathrm{s}\right)\frac{\partial u}{\partial x} + \tau_\mathrm{s}\pi\left(d_\mathrm{i} + d_\mathrm{o}\right).$$

$$\bar{M}_{xx} = \int_\mathrm{s} \sigma^s_{xx} z ds = \frac{\left(\lambda_\mathrm{s} + 2\mu_\mathrm{s}\right)\pi\left(d_\mathrm{i}^3 + d_\mathrm{o}^3\right)}{8}\frac{\partial \psi}{\partial x},$$
$$\bar{Q}_x = \int_\mathrm{s} \sigma^s_{xz}\mathrm{d}s = \tau_\mathrm{s}\pi\left(d_\mathrm{i} + d_\mathrm{o}\right)\frac{\partial w}{\partial x}. \tag{10b}$$

where k_s denotes shear correction factor. Additionally, for the kinetic energy of nanotube Π_T and the fluid kinetic energy Π_{T_f}, one can write

$$\Pi_T = \frac{1}{2}\int_x \left\{\left[\rho A + \pi\left(d_\mathrm{i} + d_\mathrm{o}\right)\rho^s\right]\left[\left(\frac{\partial u}{\partial t}\right)^2 + \left(\frac{\partial w}{\partial t}\right)^2\right] + \left[\rho I + \frac{\pi\rho_\mathrm{s}\left(d_\mathrm{i}^3 + d_\mathrm{o}^3\right)}{8}\right]\left(\frac{\partial \psi}{\partial t}\right)^2\right\}\mathrm{d}x \tag{11a}$$

$$\Pi_{T_\mathrm{f}} = \frac{1}{2}\int_0^L \int_{A_\mathrm{f}} \rho_\mathrm{f}\left\{\left(\frac{\partial w}{\partial t} + V\frac{\partial w}{\partial x}\right)^2\right.$$

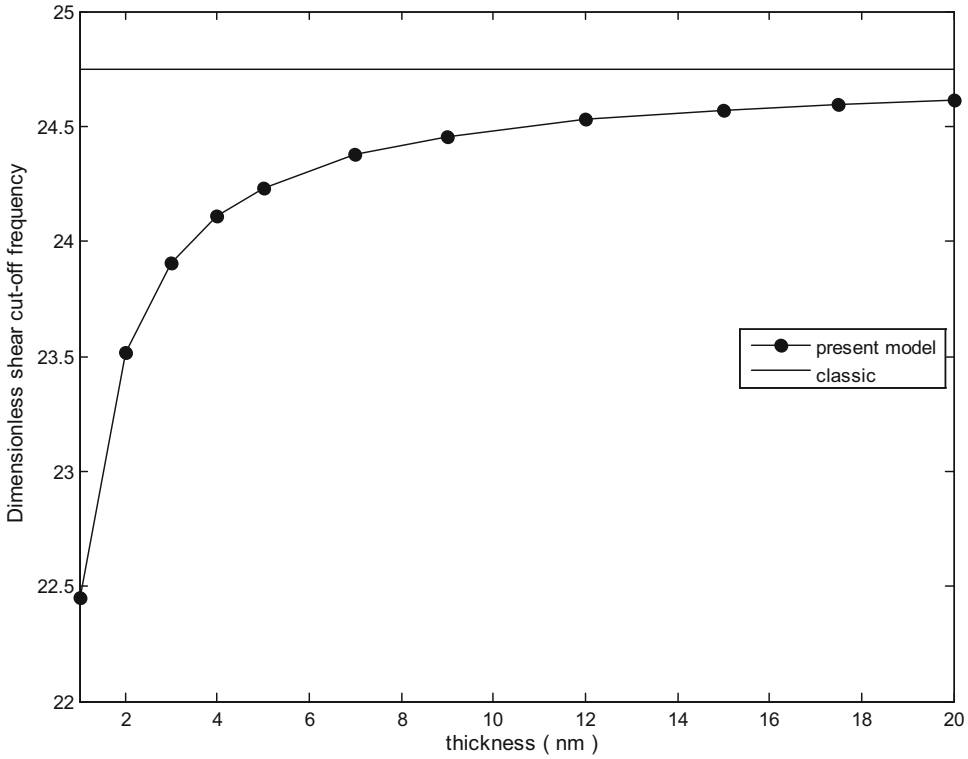

Fig. 3 Shear cutoff frequency variation with thickness

$$+\left(\frac{\partial u}{\partial t}-z\frac{\partial \psi}{\partial t}+V\right)^2\Bigg\}\mathrm{d}A_\mathrm{f}\mathrm{d}x$$

$$=\frac{1}{2}\int_0^L\Bigg\{\rho_\mathrm{f}A_\mathrm{f}\left(\frac{\partial w}{\partial t}+V\frac{\partial w}{\partial x}\right)^2+\rho_\mathrm{f}A_\mathrm{f}\left(\frac{\partial u}{\partial t}\right)^2+\rho_\mathrm{f}A_\mathrm{f}V^2+2\rho_\mathrm{f}A_\mathrm{f}\frac{\partial u}{\partial t}+\rho_\mathrm{f}I_\mathrm{f}\left(\frac{\partial \psi}{\partial t}\right)^2\Bigg\}\mathrm{d}x \tag{11b}$$

According to the Hamilton principle, one can write

$$\delta\int_{t_1}^{t_2}(\Pi_T+\Pi_{T_\mathrm{f}}-\Pi_\mathrm{s})\mathrm{d}t=0 \tag{12}$$

By taking the variation of u, w and ψ, integrating by parts and setting the coefficients of δu, δw and $\delta\psi$ equal to zero, the governing equations of motion (13a–13c) will be achieved as

$$\frac{\partial\left(N_{xx}+\bar{N}_{xx}\right)}{\partial x}=\left(\rho A+\rho_\mathrm{f}A_\mathrm{f}+\pi\left(d_\mathrm{i}+d_\mathrm{o}\right)\rho^s\right)\frac{\partial^2 u}{\partial t^2} \tag{13a}$$

$$\frac{\partial\left(Q_x+\bar{Q}_x\right)}{\partial x}-\rho_\mathrm{f}A_\mathrm{f}\left(2V\frac{\partial^2 w}{\partial t\partial x}+V^2\frac{\partial^2 w}{\partial x^2}\right)=\left(\rho A+\rho_\mathrm{f}A_\mathrm{f}+\pi\left(d_\mathrm{i}+d_\mathrm{o}\right)\rho^s\right)\frac{\partial^2 w}{\partial t^2} \tag{13b}$$

$$\frac{\partial\left(M_{xx}+\bar{M}_{xx}\right)}{\partial x}-Q_x=\left\{\rho I+\rho_\mathrm{f}I_\mathrm{f}+\frac{\pi\rho^s\left(d_\mathrm{i}^3+d_\mathrm{o}^3\right)}{8}\right\}\frac{\partial^2\psi}{\partial t^2} \tag{13c}$$

also the boundary conditions are as follows

$$\delta u=0\quad or\quad \delta\left(N_{xx}+\bar{N}_{xx}\right)=0 \tag{14a}$$

$$\delta w=0\quad or\quad \delta\left(Q_x+\bar{Q}_x\right)=0 \tag{14b}$$

$$\delta\psi=0\quad or\quad \delta\left(M_{xx}+\bar{M}_{xx}\right)=0 \tag{14c}$$

As for the stiffness components and inertia related terms, one can define

$$\begin{aligned}
&A_{11}=(\lambda+2\mu)A+\pi\left(d_\mathrm{i}+d_\mathrm{o}\right)(\lambda_\mathrm{s}+2\mu_\mathrm{s}),\\
&A_{33}=\pi\left(d_\mathrm{i}+d_\mathrm{o}\right)\tau_\mathrm{s},\ A_{55}=\mu k_\mathrm{s}A,\\
&D_{11}=(\lambda+2\mu)I+\frac{(\lambda_\mathrm{s}+2\mu_\mathrm{s})\pi\left(d_\mathrm{i}^3+d_\mathrm{o}^3\right)}{8},\\
&E_{11}=\frac{2\nu I\tau_\mathrm{s}}{(1-\nu)h}\\
&I_0=\rho A+\rho_\mathrm{f}A_\mathrm{f}+\pi\rho^s\left(d_\mathrm{i}+d_\mathrm{o}\right),\\
&I_2=\rho I+\frac{\pi\rho^s\left(d_\mathrm{i}^3+d_\mathrm{o}^3\right)}{8},\ G=\frac{2\nu I\rho^s}{(1-\nu)h}
\end{aligned} \tag{15}$$

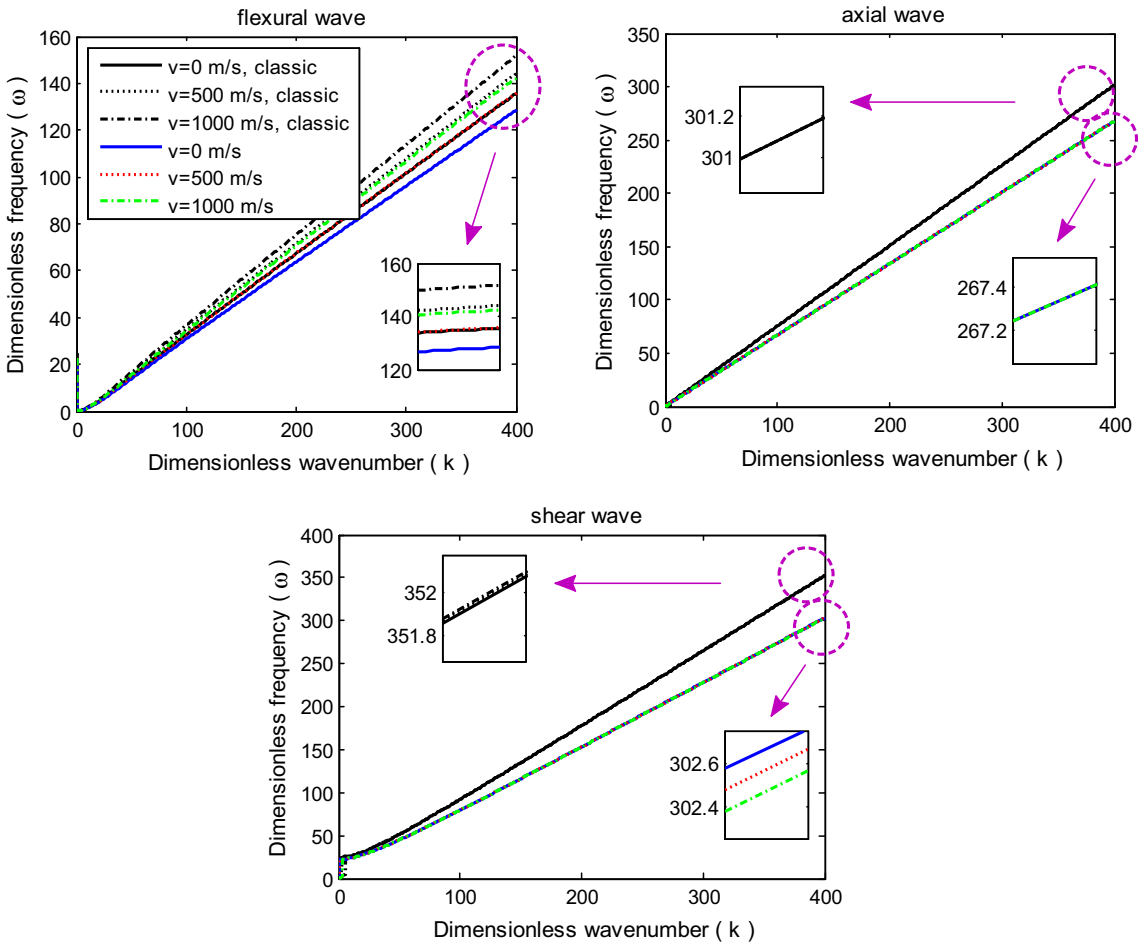

Fig. 4 Dispersion curves for different velocities corresponding to flexural, axial and shear waves

Considering above parameters and substituting Eq. (10) into (13) leads to the governing differential equations of motion as follows

$$A_{11}\frac{\partial^2 u}{\partial x^2} = I_0\frac{\partial^2 u}{\partial t^2}, A_{55}\left(\frac{\partial^2 w}{\partial x^2}+\frac{\partial \psi}{\partial x}\right) + A_{33}\frac{\partial^2 w}{\partial x^2} - \rho_f A_f\left(2V\frac{\partial^2 w}{\partial x \partial t}+V^2\frac{\partial^2 w}{\partial x^2}\right) = I_0\frac{\partial^2 w}{\partial t^2}, \tag{16a}$$

$$D_{11}\frac{\partial^2 \psi}{\partial x^2}+E_{11}\frac{\partial^3 w}{\partial x^3}-A_{55}\left(\frac{\partial w}{\partial x}+\psi\right) = I_2\frac{\partial^2 \psi}{\partial t^2}+G\frac{\partial^3 w}{\partial x \partial t^2}. \tag{16b}$$

One can introduce the following dimensionless quantities

$$u \to \frac{u}{h}, w \to \frac{w}{h}, x \to \frac{x}{L}, \eta = \frac{L}{h}, \tau = \frac{t}{L}\sqrt{\frac{A_{110}}{I_{00}}},$$

$$I_0^* = \frac{I_0}{I_{00}}, I_2^* = \frac{I_2}{I_{00}h^2}, g = \frac{G}{I_{00}h^2},$$

$$\{a_{11}, a_{13}, a_{33}\} = \left\{\frac{A_{11}}{A_{110}}, \frac{A_{13}}{A_{110}}, \frac{A_{33}}{A_{110}}\right\},$$

$$d_{11} = \frac{D_{11}}{A_{110}h^2}, e_{11} = \frac{E_{11}}{A_{110}h^2},$$

$$K_b = \frac{2\rho_f A_f V}{\sqrt{A_{110}I_{00}}}, v = \sqrt{\frac{\rho_f A_f}{A_{110}}}V \tag{17}$$

where $A_{110} = (\lambda + 2\mu)\, A$, and $I_{00} = \rho A$. Following are the normalized governing equations of motion of the nanotube

$$a_{11}\frac{\partial^2 u}{\partial x^2} = I_0^*\frac{\partial^2 u}{\partial \tau^2}, \tag{18a}$$

$$a_{55}\left(\frac{\partial^2 w}{\partial x^2}+\eta\frac{\partial \psi}{\partial x}\right)+a_{33}\frac{\partial^2 w}{\partial x^2} - K_b\frac{\partial^2 w}{\partial x \partial \tau} - v^2\frac{\partial^2 w}{\partial x^2} = I_0^*\frac{\partial^2 w}{\partial \tau^2}, \tag{18b}$$

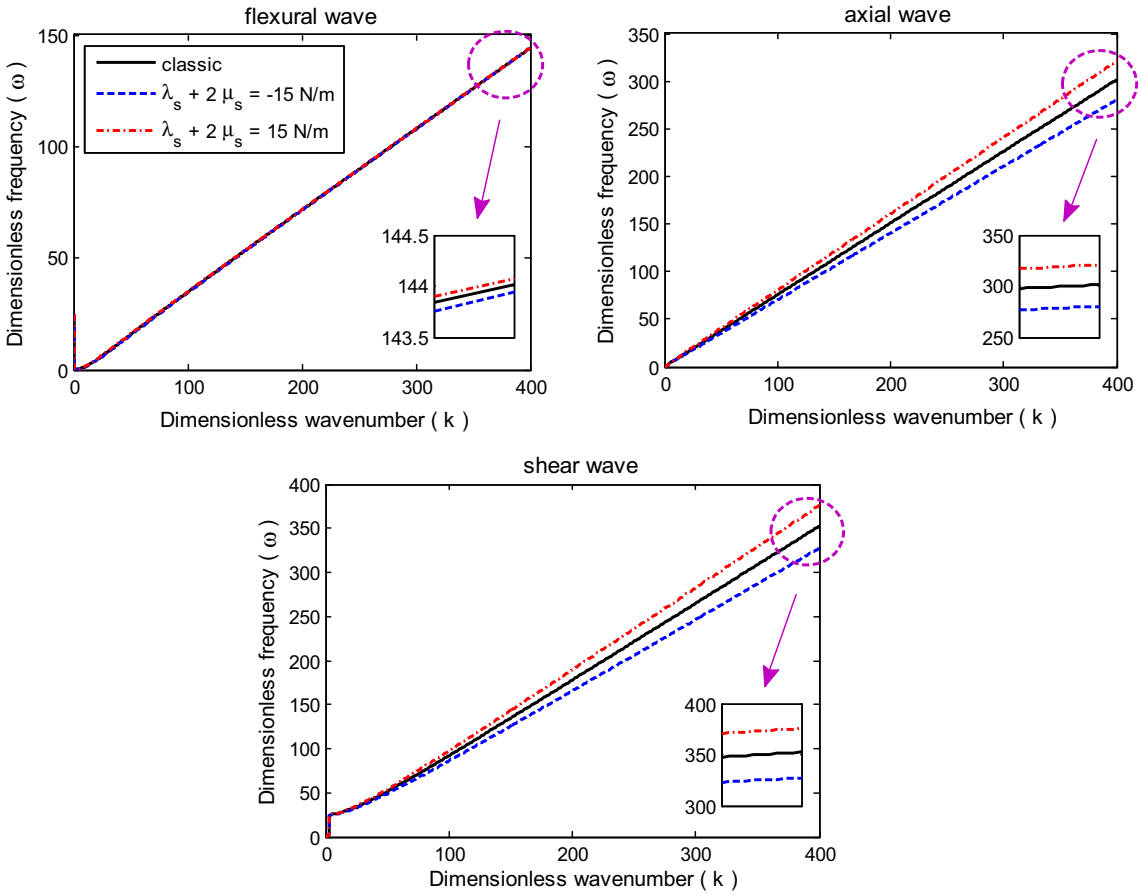

Fig. 5 Effect of the surface elastic constants on the spectrum curve for flexural, axial, and shear waves

$$d_{11}\frac{\partial^2\psi}{\partial x^2}+\frac{e_{11}}{\eta}\frac{\partial^3 w}{\partial x^3}-a_{55}\eta\left(\frac{\partial w}{\partial x}+\eta\psi\right)=I_2^*\frac{\partial^2\psi}{\partial\tau^2}+\frac{g}{\eta}\frac{\partial^3 w}{\partial x\partial\tau^2}. \tag{18c}$$

The simply supported (SS) and clamped (C) boundary conditions can be written respectively as

$$u=w=\frac{e_{11}}{\eta}\frac{\partial^2 w}{\partial x^2}+d_{11}\frac{\partial\psi}{\partial x}=0 \tag{19a}$$

$$u=w=\psi=0 \tag{19b}$$

3 Numerical Solution

To analyze the surface stress effect on the wave characteristics of nanotubes conveying fluid, the harmonic waves can be expressed as [35]:

$$u(x,t)=Ue^{i(kx-\omega t)},\ w(x,t)=We^{i(kx-\omega t)},\ \psi(x,t)=\Psi e^{i(kx-\omega t)} \tag{20}$$

where k denotes the dimensionless wave number and ω is the dimensionless frequency and U, W and Ψ are the frequency amplitude of axial and lateral deflection and rotational wave, respectively.

By substituting Eq. (20) into (18), one can obtain the following three equations of motion

$$-a_{11}k^2U+I_0^*\omega^2U=0, \tag{21a}$$

$$a_{55}\left(-k^2W+i\eta k\Psi\right)-a_{33}k^2W-K_bk\omega W+v^2k^2W+I_0^*\omega^2W=0, \tag{21b}$$

$$-d_{11}k^2\Psi-i\frac{e_{11}}{\eta}k^3W-a_{55}\eta\left(ikW+\eta\Psi\right)+I_2^*\omega^2\Psi+i\frac{g}{\eta}k\omega^2W=0 \tag{21c}$$

These equations can be expressed in the following form:

$$\left(\mathbf{M}\omega^2+\mathbf{C}\,\omega+\mathbf{K}\right)\begin{bmatrix}U\\W\\\Psi\end{bmatrix}=0 \tag{22}$$

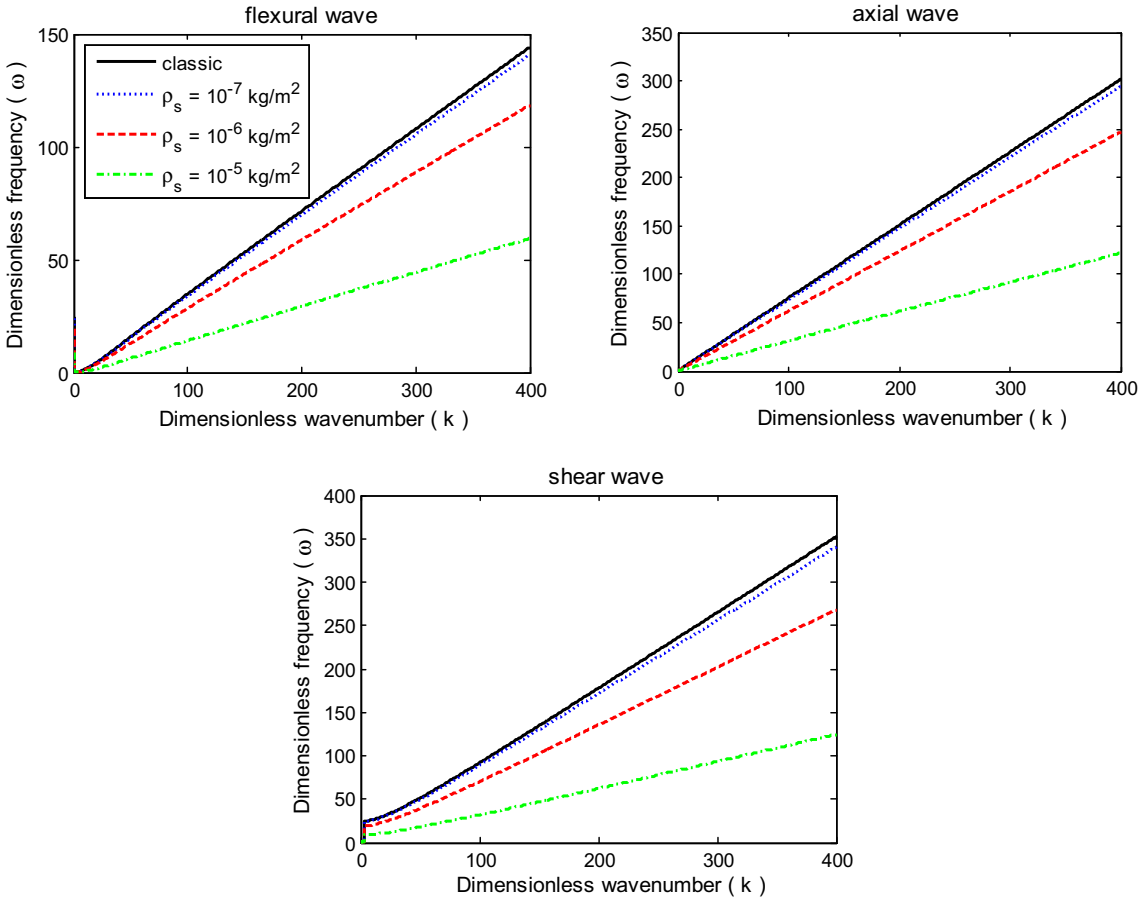

Fig. 6 Effect of the surface density on the spectrum curve for flexural, axial and shear waves

where

$$\mathbf{M} = \begin{bmatrix} I_0^* & 0 & 0 \\ 0 & I_0^* & 0 \\ 0 & i\frac{g}{\eta}k & I_2^* \end{bmatrix}, \mathbf{C} = \begin{bmatrix} 0 & 0 & 0 \\ 0 & -K_b k & 0 \\ 0 & 0 & 0 \end{bmatrix},$$
$$\mathbf{K} = \begin{bmatrix} -a_{11}k^2 & 0 & 0 \\ 0 & -a_{55}k^2 - a_{33}k^2 + v^2k^2 & a_{55}i\ \eta k \\ 0 & -i\frac{e_{11}}{\eta}k^3 - a_{55}\eta i\ k & -d_{11}k^2 - a_{55}\eta^2 \end{bmatrix} \tag{23}$$

For non-trivial solution, the determinant of the coefficient matrix in Eq. (22) must be zero which can be written in this form:

$$det\ (\mathbf{S} - \omega\mathbf{I}) = 0 \tag{24}$$

in which

$$\mathbf{S} = \begin{bmatrix} 0 & \mathbf{I} \\ -\mathbf{M}^{-1}\mathbf{K} & -\mathbf{M}^{-1}\mathbf{C} \end{bmatrix} \tag{25}$$

4 Results and Discussion

In this part, the numerical analysis is performed and results predicted by both classical and non-classical theories are illustrated in frequency versus wavenumber plots. The effects of the surface stress on the first three fundamental modes including flexural, axial, and shear waves of nanotubes are investigated. The results are presented for nanotubes made of silicon material with the following material properties [36,37]:

$$E = 210\,\text{GPa}, \rho = 2331\,\text{kg/m}^3, \nu = 0.24,$$
$$\lambda_s = -4.488\,\text{N/m}, \mu_s = -2.774\,\text{N/m}, \tau_s = 0.605\,\text{N/m},$$
$$\rho_s = 3.17e-7\,\text{kg/m}^2.$$

Figure 2 shows the variation of the wavenumber with the wave frequency of nanotubes for different thicknesses based on the present and classical beam theories. It is assumed that $d_i/d_o = 0.8, L/d_o = 20, V = 500$ m/s. It can be seen that the wave frequency gently increases with increas-

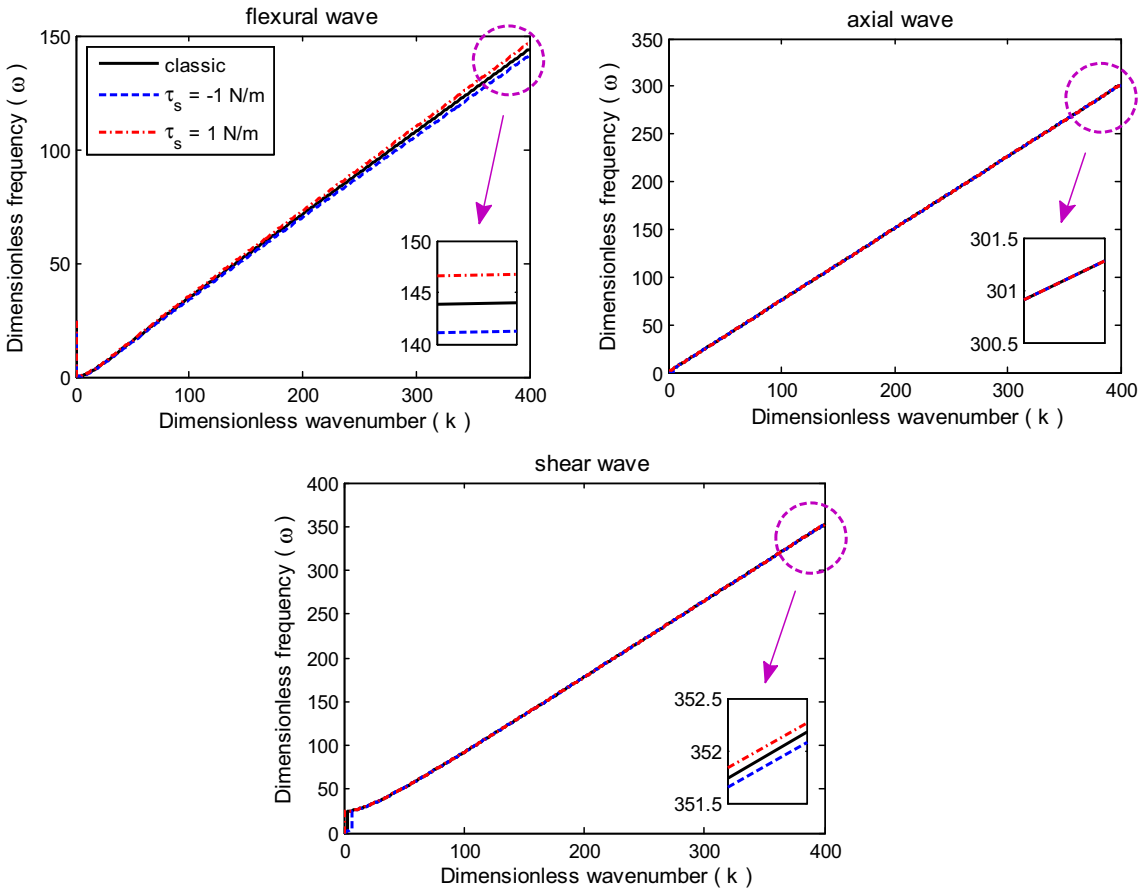

Fig. 7 Effect of the surface residual stress on the spectrum curve for flexural, axial and shear waves

ing the wavenumber. Considering the surface effects, it is observed that with the growing of the wavenumber, the distance between graphs increases. The frequencies obtained by the present model for different thicknesses are lower than those from the classical model, especially for nanotubes with smaller thicknesses. So, the small-scale effect is more pronounced for nanotubes with lower thicknesses and in higher wavenumbers. Also, it is seen that flexural and axial wave modes start from zero wave frequency, while the shear wave mode does not. The frequency at where the imaginary part of wavenumber becomes real is called as shear cutoff frequency. The cutoff frequencies can be obtained by setting $k = 0$ [38].

The dimensionless shear cutoff frequencies obtained from the present and classic models as function of thicknesses are illustrated in Fig. 3. It is observed that shear cutoff frequencies in lower thicknesses predicted by the present model are significantly smaller than those predicted by the classical theory, indicating profound effect of surface stress on the shear cutoff frequency. As it is expected, with increasing the nanotube thickness, shear cutoff frequencies of present theory get closer to those of the classical model. So, it is concluded that the classical theory can be appropriately used for nanotubes with large scales, while using this theory may lead to enormous errors in predicting the behavior of nanotubes with small scales.

Figure 4 displays the effects of surface stress and velocity on the spectrum curves with various wave modes. In all kinds of wave modes, it can be seen a significant difference between the curves with surface stress and the classical ones. At a specific velocity, the wave frequencies obtained by the present theory are lower than those predicted by the classical theory, i.e., the classical theory overestimates the wave frequency, especially at higher wavenumbers. Comparing the results of different wave modes reveals that in the flexural mode, there is most difference between curves with different velocities, while in the axial wave mode, the velocity change has almost no effect on the spectrum curve of the nanotube. It is worthwhile mentioning that in flexural and shear wave curves, the wave frequency of classical-based theory increases with increasing the flow velocity, but completely reversed behavior is observed for results predicted by present model at shear mode. Moreover, the flexural wave frequencies tend to decrease as an increase in the fluid velocity occurs. This means that increasing the fluid velocity makes the nanotubes more flexible.

Represented in Fig. 5 is the influence of the material and surface stress modulus on the spectrum curves of nanotubes with the assumption of $\rho_s = \tau_s = 0, h = 1$ nm and $V = 500$ m/s. As the wavenumber grows, the effect of the material and surface stress modulus get more pronounced, especially in axial and shear wave modes. In all three types of wave modes, the positive value of $\lambda_s + 2\mu_s$ increases the stiffness and wave frequency of the nanotube [39], while the negative one makes the structure softer and decreases the natural frequency.

The effect of the surface density on spectrum curves with the assumption of $\lambda_s = \mu_s = \tau_s = 0, h = 1$ nm and $V = 500$ m/s is depicted in Fig. 6. The frequency of the present model is smaller than that obtained by classical model and with increasing the density, this difference is growing up. For example, in flexural wave spectrum, the frequency predicted by the classical model in $k = 400$ is 2.4282 times than predicted by present theory at $\rho_s = 10^{-5}$ kg/m^2. Also it is observed that there is a significant reduction in shear cutoff frequency with increasing the surface density.

Figure 7 represents the effect of the surface residual stress on the spectrum curves with the assumption of $\lambda_s = \mu_s = \rho_s = 0, h = 1$ nm and $V = 500$ m/s. It can be seen that the influence of the surface residual stress on the spectrum curves in axial wave mode is negligible. A more difference can be observed between curves in other two wave modes in a way that with the positive value of surface residual stress, the frequency is increased while the negative one decreases the frequency.

5 Conclusion

Represented in this study was an investigation on exploring the surface stress effect on wave properties of a nanotube conveying fluids. Based on the Timoshenko beam theory and Gurtin–Murdoch continuum elasticity, a continuum model capable of capturing surface stress effect was developed. Based on the Hamilton principle, the governing equations of motion were derived, before solving numerically. Afterward, effects of the thickness, material and surface stress modulus, residual surface stress, surface density and flow velocity on wave characteristics of nanotubes predicted by both classical and non-classical theories were studied. The first three fundamental modes including flexural, axial and shear waves of nanotubes are considered.

Given the effect of the thickness, it was seen that the surface have pronounced effect on the spectrum curve of nanotubes, especially those with lower thicknesses and at higher wavenumbers. The surface stress was seen to have considerable effect on the shear cutoff frequency, especially in lower thicknesses.

Regarding the effect of the flow velocity, it was observed that depending on the type of the wave mode, the response of the spectrum curve of the nanotube can be different. For the case of the flexural mode, the variation of the velocity does not affect the spectrum curve of the nanotube. The classical theory overestimates the wave frequency, especially at higher wavenumbers. In flexural and shear wave curves, as the flow velocity rises, the wave frequency predicted by the classical theory increases, but that predicted by the present model reduces. With the increase in the wavenumber, the effect of the material and surface stress modulus was seen to be more profound, especially in axial and shear wave modes. Unlike the negative value of $\lambda_s + 2\mu_s$, the positive value of $\lambda_s + 2\mu_s$ increases the stiffness and wave frequency of the nanotube. The shear cutoff frequency was seen to be significantly decreased with increasing the surface density. As for the effect of the surface residual stress, the spectrum curve in axial wave mode was indifferent to the variation of this parameter, while in axial and flexural wave modes, the positive value of the surface residual stress slightly increases the frequency.

References

1. Iijima, S.: Helical microtubules of graphitic carbon. Nature **354**, 56–58 (1991)
2. Zhang, W.D.; Wen, Y.; Min Liu, S.; Tjiu, W.C.; Qin Xu, G.; Ming Gan, L.: Synthesis of vertically aligned carbon nanotubes on metal deposited quartz plates. Carbon **40**, 1981–1989 (2002)
3. Liu, L.; Zhang, Y.: Multi-wall carbon nanotube as a new infrared detected material. Sens. Actuators A Phys. **116**, 394–397 (2004)
4. Yan, X.B.; Chen, X.J.; Tay, B.K.; Khor, K.A.: Transparent and flexible glucose biosensor via layer-by-layer assembly of multiwall carbon nanotubes and glucose oxidase. Electrochem. Commun. **9**, 1269–1275 (2007)
5. Zhao, C.; Song, Y.; Ren, J.; Qu, X.: A DNA nanomachine induced by single-walled carbon nanotubes on gold surface. Biomaterials **30**, 1739–1745 (2009)
6. Qin, C.; Shen, J.; Hu, Y.; Ye, M.: Facile attachment of magnetic nanoparticles to carbon nanotubes via robust linkages and its fabrication of magnetic nanocomposites. Compos. Sci. Technol. **69**, 427–431 (2009)
7. Hummer, G.; Rasaiah, J.C.; Noworyta, J.P.: Water conduction through the hydrophobic channel of a carbon nanotube. Nature **414**, 188–190 (2001)
8. Gao, Y.; Bando, Y.: Nanotechnology: carbon nanothermometer containing gallium. Nature **415**, 599–599 (2002)
9. Adali, S.: Variational principles for transversely vibrating multiwalled carbon nanotubes based on nonlocal Euler–Bernoulli beam model. Nano Lett. **9**, 1737–1741 (2009)
10. Foldvari, M.; Bagonluri, M.: Carbon nanotubes as functional excipients for nanomedicines: II. Drug delivery and biocompatibility issues. Nanomed. Nanotechnol. Biol. Med. **4**, 183–200 (2008)
11. Rashidi, V.; Mirdamadi, H.R.; Shirani, E.: A novel model for vibrations of nanotubes conveying nanoflow. Comput. Mater. Sci. **51**, 347–352 (2012)
12. Stölken, J.S.; Evans, A.G.: A microbend test method for measuring the plasticity length scale. Acta Mater. **46**, 5109–5115 (1998)

13. McFarland, A.W.; Colton, J.S.: Role of material microstructure in plate stiffness with relevance to microcantilever sensors. J. Micromech. Microeng. **15**, 1060 (2005)
14. Kong, S.; Zhou, S.; Nie, Z.; Wang, K.: The size-dependent natural frequency of Bernoulli–Euler micro-beams. Int. J. Eng. Sci. **46**, 427–437 (2008)
15. Streitz, F.H.; Cammarata, R.C.; Sieradzki, K.: Surface-stress effects on elastic properties. I. Thin metal films. Phys. Rev. B **49**, 10699–10706 (1994)
16. Dingreville, R.; Qu, J.; Mohammed, C.: Surface free energy and its effect on the elastic behavior of nano-sized particles, wires and films. J. Mech. Phys. Solids **53**, 1827–1854 (2005)
17. He, J.; Lilley, C.M.: Surface effect on the elastic behavior of static bending nanowires. Nano Lett. **8**, 1798–1802 (2008)
18. Wang, G.F.; Feng, X.Q.: Effects of surface stresses on contact problems at nanoscale. J. Appl. Phys. **101**, 013510 (2007)
19. Mindlin, R.D.; Tiersten, H.F.: Effects of couple-stresses in linear elasticity. Arch. Ration. Mech. Anal. **11**, 415–448 (1962)
20. Eringen, A.C.: Nonlocal polar elastic continua. Int. J. Eng. Sci. **10**, 1–16 (1972)
21. Lam, D.C.C.; Yang, F.; Chong, A.C.M.; Wang, J.; Tong, P.: Experiments and theory in strain gradient elasticity. J. Mech. Phys. Solids **51**, 1477–1508 (2003)
22. Ansari, R.; Faghih Shojaei, M.; Gholami, R.; Mohammadi, V.; Darabi, M.: Thermal postbuckling behavior of size-dependent functionally graded Timoshenko microbeams. Int. J. Non Linear Mech. **50**, 127–135 (2013)
23. Ansari, R.; Faghih Shojaei, M.; Mohammadi, V.; Gholami, R.; Darabi, M.A.: Buckling and postbuckling behavior of functionally graded Timoshenko microbeams based on the strain gradient theory. J. Mech. Mater. Struct. **7**, 931–949 (2013)
24. Ansari, R.; Gholami, R.; Darabi, M.A.: A nonlinear Timoshenko beam formulation based on strain gradient theory. J. Mech. Mater. Struct. **7**, 195–211 (2012)
25. Ansari, R.; Gholami, R.; Shojaei, M.F.; Mohammadi, V.; Darabi, M.: Surface stress effect on the pull-in instability of hydrostatically and electrostatically actuated rectangular nanoplates with various edge supports. J. Eng. Mater. Technol. **134**, 041013 (2012)
26. Ghayesh, M.H.: Nonlinear size-dependent behaviour of single-walled carbon nanotubes. Appl. Phys. A **117**, 1393–1399 (2014)
27. Gurtin, M.; Ian Murdoch, A.: A continuum theory of elastic material surfaces. Arch. Ration. Mech. Anal. **57**, 291–323 (1975)
28. Gurtin, M.E.; Ian Murdoch, A.: Surface stress in solids. Int. J. Solids Struct. **14**, 431–440 (1978)
29. Shenoy, V.B.: Atomistic calculations of elastic properties of metallic fcc crystal surfaces. Phys. Rev. B **71**, 094104 (2005)
30. Weissmüller, J.; Cahn, J.W.: Mean stresses in microstructures due to interface stresses: a generalization of a capillary equation for solids. Acta Mater. **45**, 1899–1906 (1997)
31. Duan, H.L.; Wang, J.; Huang, Z.P.; Karihaloo, B.L.: Size-dependent effective elastic constants of solids containing nano-inhomogeneities with interface stress. J. Mech. Phys. Solids **53**, 1574–1596 (2005)
32. Sharma, P.; Ganti, S.: Size-dependent Eshelby's tensor for embedded nano-inclusions incorporating surface/interface energies. J. Appl. Mech. **71**, 663–671 (2004)
33. Wang, L.: Vibration analysis of fluid-conveying nanotubes with consideration of surface effects. Phys. E Low Dimens. Syst. Nanostruct. **43**, 437–439 (2010)
34. Lu, P.; He, L.H.; Lee, H.P.; Lu, C.: Thin plate theory including surface effects. Int. J. Solids Struct. **43**, 4631–4647 (2006)
35. Yoon, J.; Ru, C.Q.; Mioduchowski, A.: Flow-induced flutter instability of cantilever carbon nanotubes. Int. J. Solids Struct. **43**, 3337–3349 (2006)
36. Zhu, R.; Pan, E.; Chung, P.W.; Cai, X.; Liew, K.M.; Buldum, A.: Atomistic calculation of elastic moduli in strained silicon. Semicond. Sci. Technol. **21**, 906 (2006)
37. Miller, R.E.; Shenoy, V.B.: Size-dependent elastic properties of nanosized structural elements. Nanotechnology **11**, 139 (2000)
38. Narendar, S.; Gopalakrishnan, S.: Terahertz wave characteristics of a single-walled carbon nanotube containing a fluid flow using the nonlocal Timoshenko beam model. Phys. E Low Dimens. Syst. Nanostruct. **42**, 1706–1712 (2010)
39. Ansari, R.; Hosseini, K.; Darvizeh, A.; Daneshian, B.: A sixth-order compact finite difference method for non-classical vibration analysis of nanobeams including surface stress effects. Appl. Math. Comput. **219**, 4977–4991 (2013)